Angular and spectral sensitivity of fly photoreceptors. II. Dependence on facet lens F-number and rhabdomere type in Drosophila

Stavenga, DG

Published in:
Journal of comparative physiology a-Neuroethology sensory neural and behavioral physiology

DOI:
10.1007/s00359-003-0390-6

Publication date:
2003

J Comp Physiol A (2003) 189: 189–202
DOI 10.1007/s00359-003-0390-6

ORIGINAL PAPER

D.G. Stavenga

Angular and spectral sensitivity of fly photoreceptors. II. Dependence on facet lens F-number and rhabdomere type in *Drosophila*

Received: 18 September 2002 / Revised: 16 December 2002 / Accepted: 20 December 2002 / Published online: 28 February 2003

Abstract A wave-optical model for the integrated facet lens-rhabdomere system of fly eyes is used to calculate the effective light power in the rhabdomeres when the eye is illuminated with a point light source or with an extended source. Two rhabdomere types are considered: the slender rhabdomeres of R7,8 photoreceptors and the wider, but tapering R1–6 rhabdomeres. The angular sensitivities of the two rhabdomere types have been calculated as a function of F-number and wavelength by fitting Gaussian functions to the effective light power. For a given F-number, the angular sensitivity broadens with wavelength for the slender rhabdomeres, but it stays approximately constant for the wider rhabdomeres. The integrated effective light power increases with the rhabdomere diameter, but it is for both rhabdomere types nearly independent of the light wavelength and F-number. The results are used to interpret the small F-number of *Drosophila* facet lenses. Presumably the small head puts a limit to the size of the facet lens and favors a short focal length.

Keywords Fruitfly · Insect vision · Light absorption · Modes · Optical waveguides · Spatial acuity

Introduction

The visual systems of animals gather optical information from the environment by the capture of incident photons with their photoreceptors. To optimize light sensitivity, spatial resolution, and/or spectral discrimination, various optical techniques are exploited, e.g., light focusing by lenses and/or reflectors, light channeling into the visual waveguides, and selective light filtering by photostable pigments. Considering the large differences between the construction of animal eyes, several solutions to the same question seem to be acceptable, indicating that the different requirements that determine an eye's structure are not mutually exclusive. The design principles of insect compound eyes which shift the balance towards one or another of the various optical tools have been discussed in several studies during the past decades (reviews Snyder 1979; Land 1981; Warrant and McIntyre 1993; Land and Nilsson 2002).

The theme of the present paper is how the optical properties of the fly eye, arguably the compound eye with the simplest optics, determine the light sensitivity of the photoreceptors. In fly eyes, small facet lenses focus light into the rhabdomeres, where the visual pigment molecules absorb light from the propagating light waves. The diffraction optics governing the focusing properties of the facet lens (Stavenga and van Hateren 1991) and the waveguide optics of the rhabdomeres (Snyder 1979; van Hateren 1989) are well understood. Furthermore, formalisms describing the integrated optics of the facet lens-rhabdomere system are also available (Barrell and Pask 1979; van Hateren 1984). Although these treatments have been somewhat incomplete, as the optics of facet lenses deviates from classical diffraction optics (Stavenga and van Hateren 1991), the deviations occurring in the diffraction patterns can be virtually neglected when treating the integrated optics of facet lens and rhabdomere (Stavenga 2003). Because the facet lens-rhabdomere system appears to be quite robust to defocusing, the rhabdomere entrance can be assumed to coincide with the facet lens' focal plane (van Hateren 1985). In this plane, the diffraction pattern of a small lens is identical to that of a classical lens, and therefore we can reliably build upon the previous work using classical diffraction theory (Pask and Barrell 1980a; van Hateren 1984).

The crucial parameter determining the facet lens optics is the F-number, i.e., the ratio of the focal length to the lens diameter (Kirschfeld 1974; Land 1981). The F-number of the facet lenses of blowfly eyes is generally about 2.0 (Stavenga et al. 1990), but locally higher va-

D.G. Stavenga
Department of Neurobiophysics, University of Groningen,
9747 AG, Groningen, The Netherlands
E-mail: stavenga@phys.rug.nl

lues were found (van Hateren 1985), and in the fruitfly, *Drosophila*, the F-number is much lower (Franceschini and Kirschfeld 1971a). Here I will investigate how the absolute light sensitivity of fly photoreceptors depends on F-number and light wavelength, specifically for the two classes of fly rhabdomeres, R1–6 and R7,8, extending the pioneering studies of Pask and Barrell (1980a, 1980b). The analysis will allow a more general insight into the main factors determining angular and spectral sensitivity. The assembled data will be used to critically assess a formula for the angular sensitivity derived by Snyder (1979), as well as to substantiate current expressions for the absolute light sensitivity (Land 1981; Warrant and Nilsson 1998). A particularly interesting case to consider is the eye of the fruitfly, *Drosophila*, as it has an extraordinarily low F-number.

Anatomy of the eye of the fruitfly, *Drosophila*

Compound eyes consist of anatomically identical units, the ommatidia. The compound eye of *Drosophila* consists of about 700 ommatidia (Franceschini and Kirschfeld 1971a; Hardie 1985), arranged in an approximately half-sphere with radius $R = 180$ μm (Franceschini and Kirschfeld 1971b). A *Drosophila* ommatidium is capped by a biconvex facet lens, with diameter $D_l = 16$ μm (Franceschini and Kirschfeld 1971b) and thickness $t = 8$ μm (Fig. 1a). Proximally to the facet lens exists the pseudocone, a clear space, and four so-called Semper cells, covering together a distance of ca 20 μm. The eight photoreceptors, R1–8, form a retinula, situated proximally to the Semper cells (Fig. 1b). The most crucial component of a photoreceptor is the rhabdomere: it contains the visual pigment molecules as well as the phototransduction machinery (Hardie and Raghu 2001). The rhabdomeres of photoreceptors R1–6 stretch the full thickness of the retinal layer, and thus have a length $L = 80$ μm (Hardie 1985). The rhabdomeres of photoreceptors R7 and R8 together make up this distance, where the rhabdomere of R8 abuts that of R7 at about 50 μm from distal (Hardie 1985). The rhabdomeres of the R1–6 photoreceptors have distally a diameter of about 2.0 μm and taper to a diameter of about 1.0 μm proximally, whilst the diameter of the R7 and R8 rhabdomeres is more or less constant, about 1.0 μm. The rhabdomeres act as optical waveguides, because their refractive index is

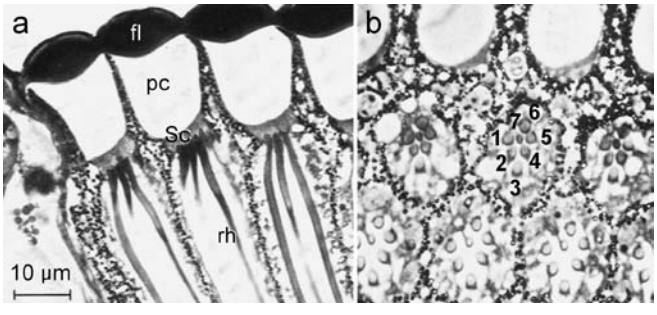

Fig. 1a,b Light microscopical sections of the eye of the fruitfly, *Drosophila* (modified from Wijngaard and Stavenga 1975). **a** Longitudinal section of a few ommatidia. An ommatidium consists, from distal to proximal, of a biconvex facet lens (*fl*), a pseudocone (*pc*), four Semper cells (*Sc*), and eight photoreceptor cells, surrounded by screening pigment cells. The rhabdomeres (*rh*), organelles that contain the visual pigment molecules, are long cylindrical structures. **b** Slightly oblique transverse cross-section, showing the pseudocone area (*top*), the distal tips of the rhabdomere area (*middle*) and a more proximal retinal area (*bottom*). The six peripheral photoreceptors (R1–6) have rhabdomeres with a distal diameter of slightly less than 2 μm (Hardie 1985), distinctly larger than the about 1 μm of the rhabdomeres of the central photoreceptors (R7,8). The R1–6 rhabdomeres extend along the full thickness of the retinal layer, and the rhabdomeres of R7 and R8 form a long cylinder with R7 distally and R8 proximally. The rhabdomeres act as optical waveguides. Their distance rapidly increases when going from distal to proximal to avoid optical cross-talk (Wijngaard and Stavenga 1975)

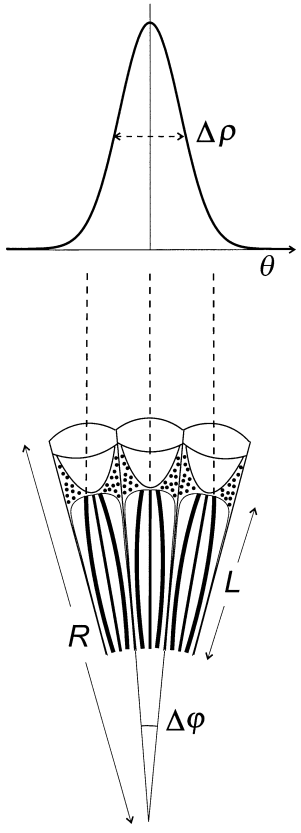

Fig. 2 Diagram of a few ommatidia of the fruitfly, *Drosophila*. The shape of the cornea, i.e., the assembly of facet lenses, is approximately a hemisphere, with radius R. The retina, i.e., the assembly of photoreceptor cells, has a thickness L. The interommatidial angle, i.e., the angle between the optical axes of adjacent ommatidia, is $\Delta\varphi$. The visual field of each photoreceptor is determined by the integrated optics of facet lens and rhabdomere. The angular sensitivity is the normalized sensitivity as a function of θ, i.e., the angle between a point in space and the photoreceptor visual axis. Its shape is generally well approximated by a gaussian, with half width $\Delta\rho$. In neighboring ommatidia, photoreceptors of a specific set share the same visual field. The *dashed lines* indicate their visual axes

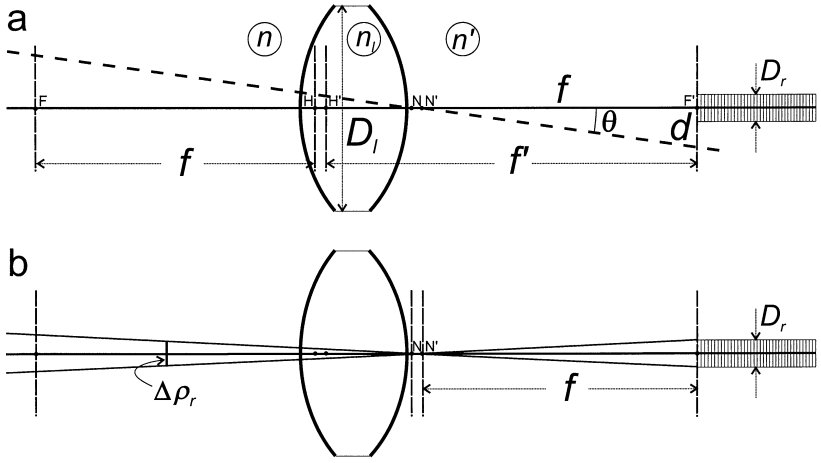

Fig. 3a,b Geometrical optics representation of the thick facet lens of *Drosophila* and a rhabdomere. **a** n, n_l, and n', refractive indices of object space, facet lens, and image space, respectively; F and F', focal points; H and H', principal points; N and N', nodal points; f and f', focal lengths, with $f' = n'f$ (the parameters without and with a prime concern the object and image space, respectively); D_l, facet lens diameter; D_r, rhabdomere diameter. Light incident from a direction θ hits the image focal plane at a distance $d = f\text{tg}\theta$ from the focal point F'. **b** When the rhabdomere entrance is at the focal plane, the diameter of the visual field according to geometrical optics is given by $\Delta\rho_r = D_r/f$

higher than that of the surrounding medium. The distance between the different rhabdomeres of an ommatidium rapidly increases from distal to proximal (Fig. 1), thus diminishing optical cross-talk (Wijngaard and Stavenga 1975).

In the fly neural superposition eye (Kirschfeld 1967), adjacent ommatidia contain specific sets of photoreceptors which have their axons joined in the same neural cartridge in the lamina, i.e., the first optic ganglion connecting the retina. These photoreceptors have identical visual axes (Fig. 2), and therefore the rhabdomeres are closely packed distally. Although the photoreceptors of a particular ommatidium have different visual axes (except for R7 and R8), the number of the eye's sampling points is identical to the number of ommatidia, and the spatial sampling lattice is hence determined by the value of the interommatidial angle $\Delta\phi = D_l/R$ (Fig. 2), yielding for *Drosophila* $\Delta\phi = 5.1°$. The photoreceptors have a restricted visual field, determined by the optical combination of the facet lens and rhabdomere. The spatial or angular sensitivity function (also called the acceptance function) is more or less Gaussian-shaped (Götz 1964), which also holds for the neurons in the lamina which receive the photoreceptor signals from those photoreceptors which share the visual field (van Hateren et al. 1989). The half width of the angular sensitivity curve is given by $\Delta\rho$ (Fig. 2). Its value for *Drosophila* has only been derived from behavioral experiments, giving a value of $\Delta\rho = 3.5°$ (Götz 1964). One of the themes of this paper is how the combined optical properties of facet lens and rhabdomere determine the angular sensitivity.

Results

Geometrical optics of the *Drosophila* facet lens and rhabdomeres

The fly facet lens is well approximated by a thick lens (Kuiper 1965; Stavenga 1975; McIntyre and Kirschfeld 1982; Stavenga et al. 1990). The thick lens is a classical case of geometrical optics (Fig. 3). The lens power, P_l, follows from the radius of curvature of both surfaces, $r_1 = -r_2 = 11 \pm 1$ μm, the thickness $t = 8 \pm 1$ μm (Fig. 1), and the refractive indices of object space, facet lens and image space, $n = 1.0$, $n_l = 1.45$ (Stavenga et al. 1990), and $n' = 1.34$ (Seitz 1968), respectively, yielding $P_l = 0.049 \pm 0.004$ μm^{-1}. The object focal length, which is equal to the posterior nodal distance (Fig. 3b), then is $f = 20 \pm 2$ μm, and the image focal length $f' = 27 \pm 3$ μm (see Appendix 1). This result fully agrees with the data derived from optical experiments, which demonstrated that the tips of the rhabdomeres coincide with the image focal plane of their facet lens and that the image focal length is 26.8 ± 2.3 μm (Franceschini and Kirschfeld 1971a, 1971b).

From these figures the F-number, $F = f/D_l$, of the *Drosophila* facet lens is $F = 1.25 \pm 0.13$. This is a much lower F-number than the $F = 1.9$ of the facet lenses of the housefly *Musca* (Stavenga 1975) or $F = 2.0 \pm 0.2$ for the blowflies *Calliphora* and *Chrysomia* (Stavenga et al. 1990). Values as high as $F = 3.0$ have been found locally for blowfly (van Hateren 1985).

The F-number has important consequences for the light capture by the rhabdomeres, as can be illustrated with geometrical optics. Figure 4 schematically presents the lens-rhabdomere system for a few F-number values. The facet lens is indicated by the secondary principal plane and the rhabdomere entrance plane is co-localized with the image focal plane. The angle between a light ray from the lens margin and the optical axis then is (Appendix 1):

$$\theta_a = \text{tg}^{-1}\left[\frac{D_l}{2f'}\right] = \text{tg}^{-1}\left[\frac{n'}{2F}\right] \quad (1)$$

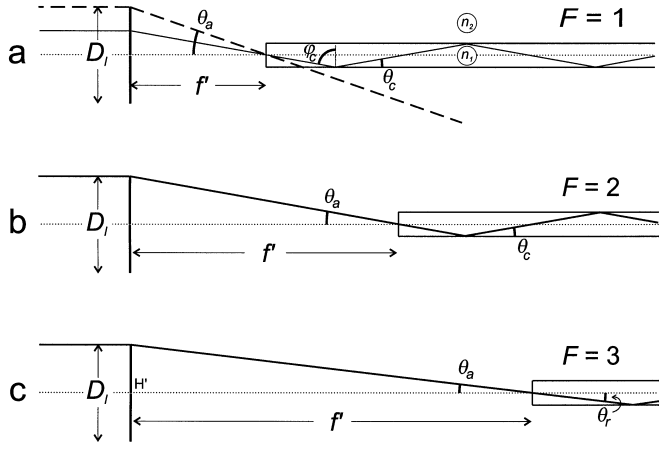

Fig. 4a–c Geometrical optics diagram of light focusing by a fly facet lens onto a rhabdomere. Three values of the lens F-number, $F=f/D_l$, 1, 2 and 3 in **a**, **b** and **c**, respectively, spanning the range found experimentally, are illustrated. The diameter of the facet lens, D_l, is assumed to be constant. The rhabdomere entrance is assumed to be located in the image focal plane. Light rays incident at the facet lens parallel to the lens-rhabdomere axis are considered. The lens aperture angle is $\theta_a = \mathrm{tg}^{-1}(D_l/2f')$. The ratio of the refractive indices of rhabdomere and surrounding medium, n_1 and n_2, respectively, determines the rhabdomere critical angle: $\phi_c = \sin^{-1}(n_2/n_1)$; its complement is $\theta_c = \cos^{-1}(n_2/n_1)$. The rhabdomere refraction angle is $\theta_r = \sin^{-1}[(n_2/n_1)\sin\theta_a]$. When $\theta_r > \theta_c$ (**a**) only part of the light rays are captured by the rhabdomere. When $\theta_r < \theta_c$ (**c**) all light rays are totally reflected at the rhabdomere border. The optimal situation occurs when $\theta_r \approx \theta_c$ (**b**): just about all light rays are channeled successfully into the rhabdomere

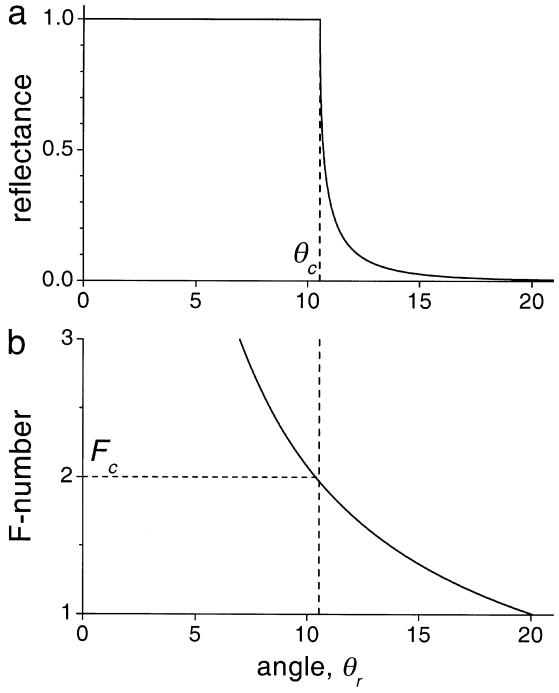

Fig. 5a,b Reflectance of the rhabdomere boundary as predicted by the Fresnel reflection equations, Appendix 2 (**a**), and relationship between the F-number of the facet lens and the angle of a marginal light ray propagating in the rhabdomere (**b**). The continuous curve in **b** is calculated from $F = 1/(2n'\mathrm{tg}\theta_a)$ with $\theta_a = \sin^{-1}[(n_1/n_2)\sin\theta_r]$. The complement of the critical angle, $\theta_c = \cos^{-1}(n_2/n_1) = 10.5°$. Light is focused efficiently into the rhabdomere by a lens with F-number $F > 2$, but when $F < 2$ light rays leaving the lens periphery are largely leaking out

The light ray is very slightly refracted when entering the rhabdomere, because the refractive index of the rhabdomere, $n_1 = 1.363$ (Beersma et al. 1982), is slightly higher than that of the surrounding medium, $n_2 = n' = 1.340$ (Seitz 1968), resulting in a rhabdomere refraction angle $\theta_r = \sin^{-1}[(n_2/n_1)\sin\theta_a]$; see Fig. 4c. When the light ray subsequently reaches the rhabdomere boundary its fate depends strongly on the incident angle. When this angle exceeds the critical angle, $\phi_c = \sin^{-1}(n_2/n_1)$, see Fig. 4a, it is totally reflected, i.e., the reflectance is equal to 1 when $\theta_r < \theta_c = 90° - \phi_c$ (Fig. 4c). However, when $\theta_r \gg \theta_c$, the light ray leaves the rhabdomere without appreciable reflection (see Fig. 5a). The transition between total reflection and virtually total light loss is very sharp, and occurs at about $F = 2$ (Appendix 2 and Fig. 5b).

The visual field of a rhabdomere according to geometrical optics is determined by the incident light rays which proceed from the secondary nodal point, N', to the rhabdomere border (Fig. 3b). The angular diameter of the rhabdomere is $\Delta\rho_r = D_r/f = D_r/D_lF$ (Fig. 3b), see also Snyder (1979). For *Drosophila*, $D_r = 2.0$ μm (R1–6) yields $\Delta\rho_r = 5.7 \pm 0.5°$, and $D_r = 1.0$ μm (R7,8) yields $\Delta\rho_r = 2.9 \pm 0.3°$.

Wave optics of the fly facet lens-rhabdomere system

Geometrical optics can only partially describe the characteristics of the optical system of the fly eye. The wave properties of light cause diffraction of the incident light, at the facet lens aperture, and the excitation of specific light distribution patterns, so-called waveguide modes, when light enters the fly rhabdomere (Snyder 1979; van Hateren 1989; Stavenga 2003). The spatial light distribution of each mode and the number of modes are determined by the waveguide number (Snyder 1979):

$$V = \frac{\pi D_r}{\lambda}\sqrt{(n_1^2 - n_2^2)} \qquad (2)$$

where λ is the light wavelength. A certain mode is allowed to propagate when $V > V_c$, the mode's cut-off value (for mode nomenclature and V_c-values, see Stavenga 2003).

Incident light entering the rhabdomere is distributed over the allowed modes depending on the light pattern at the rhabdomere entrance and the mode patterns. The sum of the light power of the different excited modes then is available for absorption by the visual pigments. The photoreceptor's light sensitivity is thus determined on one hand by the light power channeled by the optics into the rhabdomere as waveguide modes and on the other hand by the visual pigments which absorb from the light that travels through the rhabdomere. Expressions for the excitation of waveguide modes have been derived by Barrell and Pask (1979) and van Hateren (1984); see Appendix 3 (Stavenga 2003).

The light power propagated in waveguide modes is distributed partially inside and outside the waveguide boundary. The fraction of the light power inside the boundary is given by $\eta_p(V)$, which is a unique function of V for each mode (Eq. A13, Appendix 3); p is the mode number. Figure 6a gives the value of η_p as a function of λ for the rhabdomeres of the photoreceptors R7 and R8, assuming a constant diameter of 1.0 μm. Throughout the visible range, only one mode is allowed. The second mode can only propagate in the far-ultraviolet. In the rhabdomeres of R1–6, with a distal diameter of 2.0 μm, 1–5 modes are allowed, depending on the wavelength (Fig. 6b). Figure 6c gives the effective light fraction $\bar{\eta}_p$ for a parabolic tapering rhabdomere (see Appendix 3).

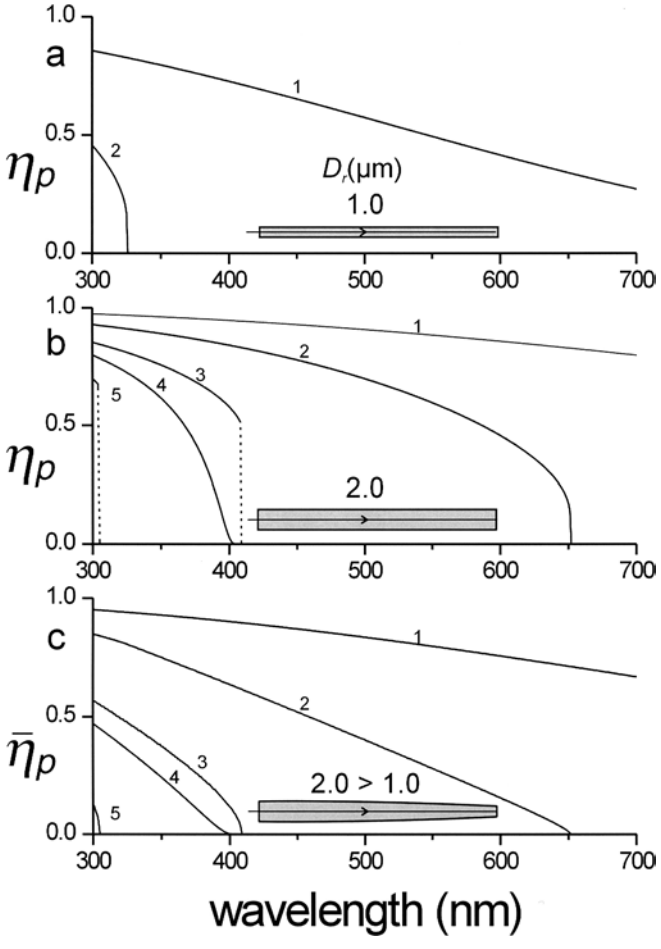

Fig. 6a–c The fraction of the light power propagated by waveguide modes within the rhabdomere boundary. When the rhabdomere diameter D_r = 1.0 μm (**a**), only the first mode is allowed, except in the far UV. The light fraction within the rhabdomere, η_p, decreases with increasing wavelength for all modes. When D_r = 2.0 μm (**b**), up to five modes are allowed at 300 nm. When the rhabdomere tapers (**c**), the effective light fraction $\bar{\eta}_p$ is the length average of η_p (Eq. A12). Parabolic tapering is assumed (see Appendix 3)

Effective light power as a function of wavelength and angle of light incidence

The light power effective for light absorption is the light power propagated inside the rhabdomere, i.e., the effective mode power is the product of the excited mode light power and the light fraction $\bar{\eta}_p$. When P_{eff} is the total effective light power, i.e., the sum over all modes, the light absorbed by the visual pigment is (Eq. A6, Appendix 3):

$$P_{abs}(\theta, \lambda) = \kappa(\lambda)\, L\, P_{eff}(\theta, \lambda) \tag{3}$$

where $\kappa(\lambda)$ is the absorption coefficient of the rhabdomere medium due to the visual pigment, and L is the length of the rhabdomere; Eq. 3 holds under the condition that self-absorption by the visual pigment is limited (Appendix 3). The angular sensitivity of a photoreceptor for a certain wavelength λ then follows from normalizing the absorbed light power, $P_{abs}(\theta,\lambda)$, or equivalently, from normalizing $P_{eff}(\theta,\lambda)$. Similarly, the spectral sensitivity for light coming from a certain direction θ (for instance the axial direction, where $\theta = 0°$) is obtained by normalizing the spectrum of absorbed light, $P_{abs}(\theta,\lambda)$.

The effective light power can be calculated from expressions for the light power excited in a waveguide mode p by a point source, derived by Barrell and Pask (1979) and van Hateren (1984). Figure 7 presents results for the two types of fly rhabdomeres as a function of incident light angle, θ, for a few wavelengths. Figures 7a–e present the case of the constant diameter R7,8 rhabdomeres and Fig. 7f–j that of the tapering R1–6 rhabdomeres. The range of the F-number of the facet lens is from 1.0 to 3.0. The angles in the abscissa of Fig. 7 refer to a fly facet lens with diameter D_l = 25 μm, typical for larger flies such as *Musca* and *Calliphora*. Because the F-number fully determines the contribution of the facet lens to P_{eff} (see Eq. A10 of Appendix 3 and Stavenga 2003), graphs of P_{eff} for the smaller *Drosophila* facet lens (D_l = 16 μm) are identical to Fig. 7 when the abscissa is multiplied with a factor 25/16.

Figure 7 shows that the effective light power strongly depends on both the F-number and the light wavelength λ. For most wavelengths, P_{eff} (θ,λ) has a more or less Gaussian dependence on the incident light angle, but severe deviations occur when $F < 2$ for the wider rhabdomere type, due to the excitation of several modes, yielding double-peaked angular sensitivity curves at short wavelengths. The thin vertical lines in Fig. 7 indicate the angular radius of the rhabdomere $\Delta\rho_r/2 = D_r/2f = D_r/2D_lF$. The angular radius changes inversely with the focal distance (f): i.e., it decreases when the rhabdomere is positioned further away from the lens (Figs. 3, 4). At variance with the prediction from geometrical optics, light excitation does not rapidly diminish when the directional angle of the light source is larger than the angular radius of the rhabdomere. This is related to the width of the diffraction pattern projected in the lens' focal plane. As

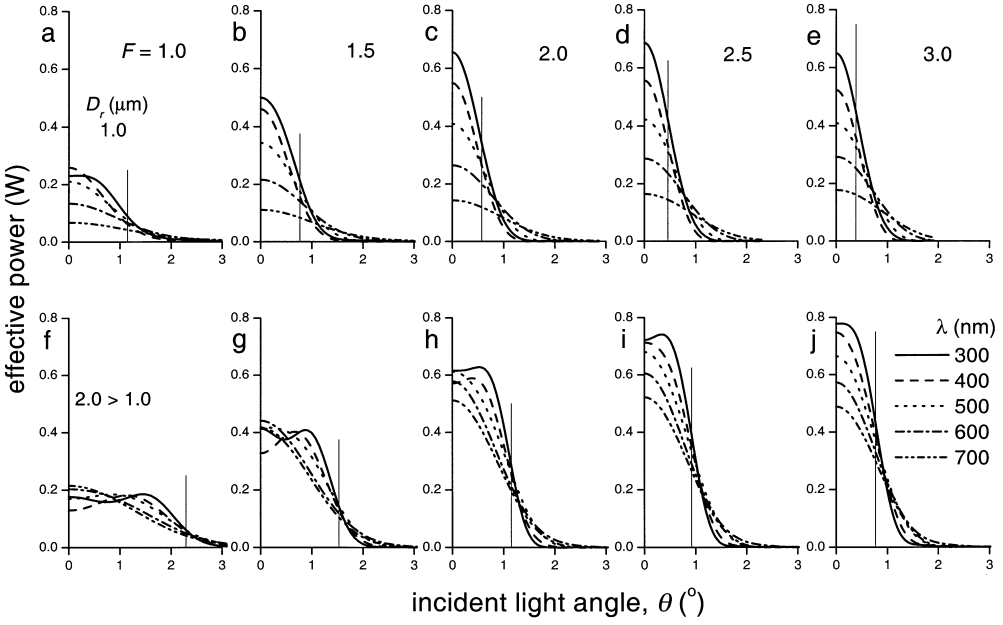

the width is proportional to the F-number, the large angular sensitivity is especially noticeable for the slender rhabdomere type (D_r = 1.0 μm) at F = 3.0 (Fig. 7e).

Effective light power with on-axis illumination

Figure 8 presents the axial effective power, i.e., when the light source is on-axis (θ = 0°), showing the dependence of the facet lens-rhabdomere system on F-number and wavelength in some more detail. In both rhabdomere types P_{eff} increases with increasing F-number, reaching a plateau at (very roughly) F = 2. Note that always the same light power of 1 W is assumed to enter the facet lens. This confirms the geometrical optics above (Appendix 2), which showed the reduced light capture when $F < 2$ and maximum light capture when $F > 2$. The severe decrease of P_{eff} with increasing wavelength (Fig. 8b, d), especially in the slender rhabdomere type (D_r = 1.0 μm), is mainly due to the wavelength dependence of the mode power fraction η_p inside the rhabdomere boundary (see Fig. 6a).

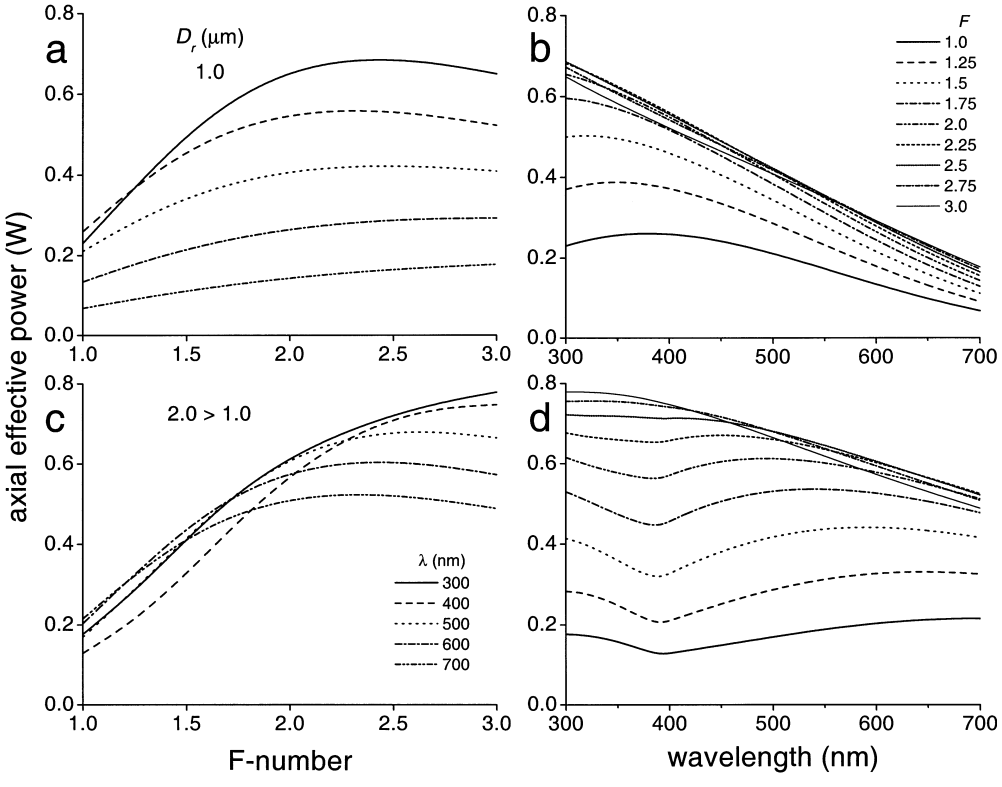

Fig. 8a–d Effective light power with on-axis illumination and 1 W of monochromatic light entering the facet lens as a function of F-number for a few wavelengths (**a**, **c**), and as a function of wavelength for a few F-numbers (**b**, **d**), for the R7,8 rhabdomere type (**a**, **b**) and for the R1–6 rhabdomere type (**c**, **d**). The effective power is low at low F-numbers, and it is about maximal for F > 2. The decrease with increasing wavelength, especially when D_r = 1.0 μm (**b**), is mainly due to the decrease in η_p with wavelength

◄

Fig. 7a–k The effective light power in the two rhabdomere types when 1 W of monochromatic light, wavelength λ, enters a facet lens with F-number F = 1.0–3.0. The *thin lines* indicate the incident light angle that is aligned with the rhabdomere boundary. The graphs hold for a facet lens diameter of D_l = 25 μm. For facet lenses with a different D_l the abscissa must be rescaled by $25/D_l$

Effective light power with an extended light source

Light capture declines severely in both rhabdomere types when $F < 2$, posing the question why the *Drosophila* facet lens has gone down to as low as F = 1.25. The answer may be gained from Fig. 7, which shows that $P_{eff}(\theta,\lambda)$ progressively broadens when F decreases. It is hence of interest to calculate the light capture from an extended light source. Figure 9 presents the integral effective power result, $P_{\text{int}}(\lambda)$, when the system is illuminated with a uniform light source emitting 1 W sr^{-1} μm^{-2} (Appendix 4). Contrary to the axial effective power, the integral effective power decreases (though only weakly) with F at all wavelengths (Fig. 9a). The severe dependence on F, apparent in the effective power with a point source (Fig. 8) is strongly suppressed with an extended light source (Fig. 9). This holds for both rhabdomere types. The amplitudes of the axial effective power only slightly differ between the two rhabdomere types (Fig. 8), but the differences are considerably enhanced in the integral effective power (Fig. 9a, b), obviously due to the broader angular curves of the wider rhabdomeres (Fig. 7).

Fig. 9a,b Integral effective power calculated for an extended, monochromatic light source with irradiance 1 W sr^{-1} μm^{-2}. The slender rhabdomere type captures less light than the wider rhabdomere. The dependencies on F-number (**a**) or wavelength (**b**) are minor

Photoreceptor spectral sensitivity

The spectral sensitivity of the photoreceptors is obtained by normalizing the absorbed light power, which is the effective light power multiplied by the visual pigment absorption coefficient and the rhabdomere length (Eq. 3; Appendices 3 and 4). The spectral dependence of the axial effective power (Fig. 8b, d) modulates the visual pigment's absorption spectrum, especially in the slender rhabdomeres, where the long wavelength part is suppressed (Fig. 8b). The spectral modulations due to the integral effective power (Fig. 9b) are relatively minor. A comparison of Figs. 6 and 9 indicates that the modulations will be largest at those wavelengths where the number of allowed modes changes.

Photoreceptor angular sensitivity

The commonly used measure for characterizing the spatial characteristics of a photoreceptor is the half width of the angular sensitivity function, $\Delta\rho$ (Fig. 2). Figure 7 shows that this function not always has the assumed Gaussian shape, but can become double-peaked. Nevertheless, Gaussian functions of the light incidence angle θ can be fitted to curves of $P_{eff}(\theta,\lambda)$ like those in Fig. 7, yielding the $\Delta\rho$-values presented in Fig. 10, for both rhabdomere types as a function of F-number for a few wavelengths (Fig. 10a, d), and as a function of wavelength for a few F-numbers (Fig. 10b, e). The data refer again to a facet lens diameter of D_l = 25 μm, but the $\Delta\rho$-curves for facet lenses with another D_l are identical when the ordinate is multiplied with $25/D_l$.

The angular sensitivity function of the photoreceptors narrows with increasing F-number, clearly due to a decrease in angular diameter of the rhabdomere (Fig. 10a, d). The photoreceptors with the slender rhabdomeres demonstrate a considerable increase of the angular sensitivity with wavelength in the range where

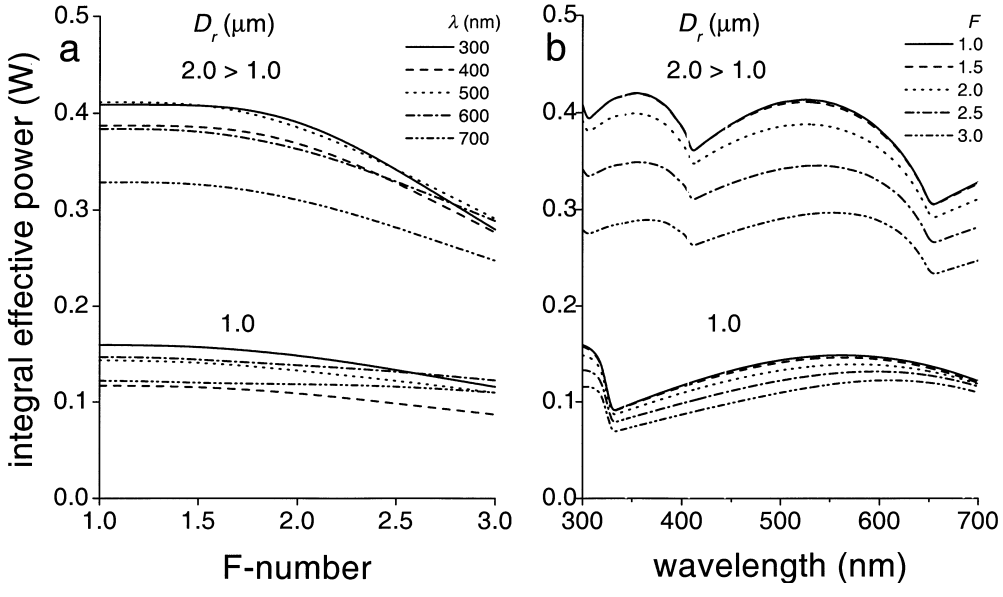

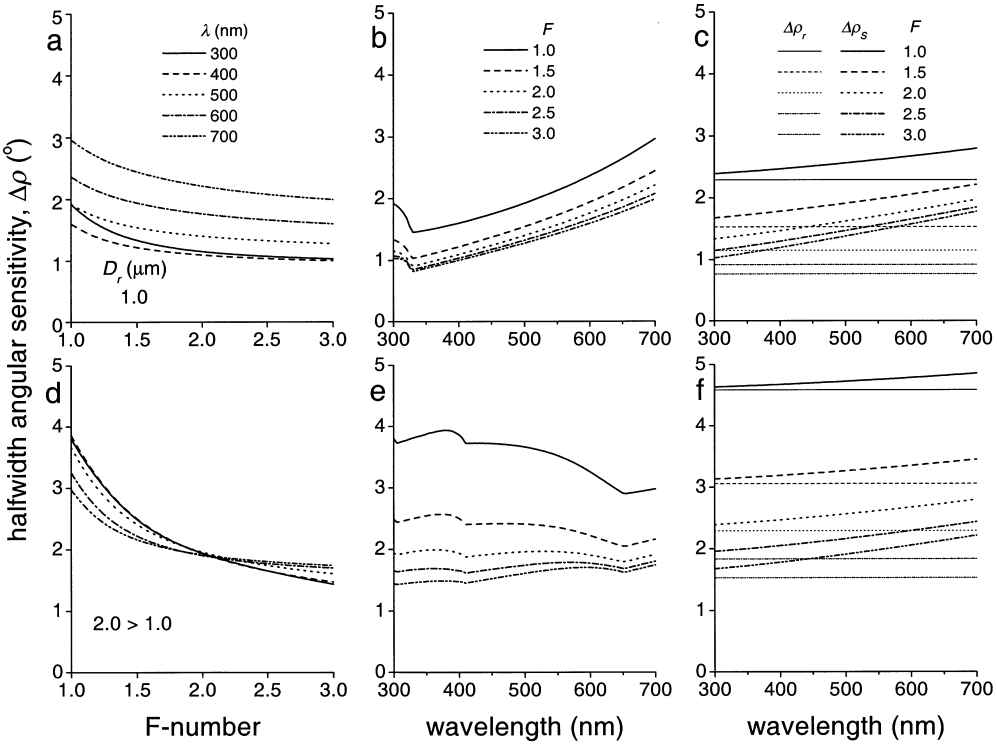

Fig. 10a–f Half width of photoreceptor angular sensitivity curves, $\Delta\rho$, calculated by fitting Gaussian functions at the effective light power functions of Fig. 7 (**a**, **b**, **d**, **e**). The data refer to a facet lens with D_l = 25 μm, i.e., for facet lenses with a different D_l the ordinate must be rescaled by $25/D_l$. For comparison, the dependence of $\Delta\rho$ on wavelength predicted by a formula derived by Snyder (1979), Eq. 4, is shown in **c** and **f**. **a**–**c** refer to the rhabdomeres with constant diameter D_r = 1.0 μm; **d**–**f** refer to the rhabdomeres with a diameter tapering parabolically from 2.0 to 1.0 μm

only the first mode is allowed (Fig. 10b), whilst the photoreceptors with the fatter rhabdomeres have a rather wavelength-independent angular sensitivity, except for a very low F-number (Fig. 10e). Figures 10b and e show characteristic modulations in the angular sensitivity at those wavelengths where the number of allowed modes changes.

Snyder (1979) derived a simple expression for the angular sensitivity of fly photoreceptors. He assumed that lens diffraction and rhabdomere acceptance both have a Gaussian dependence on the angle of light incidence and that the Gaussians are additive, resulting in an angular sensitivity function with half width:

$$\Delta\rho_S = \sqrt{\Delta\rho_l^2 + \Delta\rho_r^2} \qquad (4)$$

where $\Delta\rho_l = \lambda/D_l$ is the half width of the Gaussian-fit to the diffraction pattern of a facet lens, and $\Delta\rho_r$ is the half width of the rhabdomere acceptance function, which is taken to be identical to the angular diameter of the rhabdomere, $\Delta\rho_r = D_r/f = D_r/D_lF$. Figures 10c and f present the data predicted by Eq. 4 for the different F-numbers and rhabdomere types. The $\Delta\rho_r$-values were calculated by using for D_r the diameter of the rhabdomeres' distal tip. Because $\Delta\rho_l$ is proportional to λ, $\Delta\rho_S$ increases monotonically with wavelength.

A comparison of $\Delta\rho$-spectra obtained from the wave optical model (Figs. 10b, e) with the corresponding predictions by Eq. 4 shows that the Snyder model is not too far off at $F \approx 2$, but in general it is quite inadequate. The reason for this failure must be sought in the essential incorrect assumptions of the model, as has already been forcefully argued by van Hateren (1984; see also Warrant and McIntyre 1993). Despite these early criticisms, Eq. 4 has prevailed ever since (e.g., Land and Nilsson 2002). Figures 10b and c indicate that Eq. 4 gives approximately the right trend for the slender rhabdomere photoreceptors (Pask and Barrell 1980a), but for the photoreceptors with the wider rhabdomeres one could just as well take $\Delta\rho$ to be a constant, equal to $\Delta\rho_r$ (see Stavenga 2003).

Discussion

Assumptions of the wave-optics model calculations

The wave properties of light play a dominant role in fly vision. Although geometrical optics is suitable for capturing the general aspects of imaging by the facet lens and light guiding by the rhabdomeres, wave optics is essential for a quantitative description of the light sensitivity of the photoreceptors. The effective light power launched into the rhabdomeres for absorption by the visual pigment has been calculated here for the two main types of rhabdomeres using the powerful formalisms developed by Barrell and Pask (1979) and van Hateren

(1984); see also Stavenga (2003). Data very similar to those of the present paper have been reported by Pask and Barrell (1980a, 1980b), though in a slightly different fashion. These two insightful papers treat a specific fly facet lens with diameter $D_l = 26$ μm, together with the same rhabdomere types used here. The dependence of light capture by the rhabdomeres has been illustrated for various situations. For instance, the on-axis data in Figs. 5–7 of Pask and Barrell (1980a) for the dependence of the light capture on wavelength and focal distance is very similar to that in the present Fig. 8. Some of Pask and Barrell's (1980a) data is repeated here in a more accessible form. An important difference of the present paper with the Pask and Barrell (1980a, 1980b) papers is the emphasis on the weighting factor imposed by the light fraction η_p on the light power in the rhabdomere. The distinct effect on the angular sensitivity has not been incorporated in most of Pask and Barrell's (1980a, 1980b) data. Figures 7 and 10 of the present paper refer to a facet lens with $D_l = 25$ μm and not explicitly to the *Drosophila* lens of $D_l = 16$ μm to emphasize that the data can be easily generalized by simply scaling the coordinates, as the relevant basic parameter is the F-number.

The excited power has been calculated assuming that the distal end of the rhabdomere coincides with the secondary focal plane of the facet lens (Eq. A7). This assumption cannot hold for all wavelengths, because facet lenses suffer from chromatic aberration (McIntyre and Kirschfeld 1982). The error involved will remain minor, however, as the facet lens-rhabdomere is quite robust to defocus (Pask and Barrell 1980a; Stavenga 2003), although some modulation of the data may not be fully negligible. It is, however, in principle straightforward to perform the calculations for the out-of-focal-plane case. The formalism of Barrell and Pask (1979) then has to be slightly modified (Stavenga 2003).

The effective light power available for light absorption, P_{eff}, is defined as the sum over all modes of the product of the excited mode power and the light fraction inside the rhabdomere, η_p (Appendix 3). The underlying assumption is that the total absorption is not excessive, so that the expression for the basically exponential absorption can be reduced to the first term (Eqs. A5 and A6, Appendix 3; see Pask and Barrell 1980a). Whether this assumption is valid depends on the value of the product $A_p = \bar{\eta}_p(\lambda)\kappa(\lambda)L$, where $\bar{\eta}_p$ is the average light fraction inside the rhabdomere, $\kappa(\lambda)$ the absorption coefficient of the rhabdomere tissue, and L the length of the rhabdomere. For a *Drosophila* R1–6 rhabdomere, in the range of the rhodopsin peak wavelength ($\lambda_{max} = 490$ nm) $\bar{\eta}_1 = 0.84$ (Fig. 3), and with $\kappa = 0.007$ μm^{-1} (Warrant and Nilsson 1998) and $L = 80$ μm we obtain $A_p = 0.47$. The linear approximation then overestimates the absorption by 9.5%. For wavelengths increasingly remote from the peak wavelength this error decreases (although it can become larger in the UV due to the strongly absorbing sensitizing pigment of R1–6 photoreceptors). The length of the central rhabdomeres, of photoreceptors R7 and R8, is 2/3 and 1/3, respectively, of the length of R1–6 rhabdomeres, and therefore the errors due to linear approximation are then smaller. The approximation will cause more severe errors in the larger flies, where $L > 200$ μm. In other words, the linear approximation of Eq. 3 can be too coarse in the peak wavelength range for the larger flies. In those cases the full formalism has to be applied (Stavenga 2003). The big advantage of the linear approximation, used in the present paper, is the segregation of the effects of facet lens and rhabdomere optics from those of the visual pigment absorption, thus allowing a ready insight into the mechanisms that determine photoreceptor sensitivity.

In normal life, fly eyes do not receive monochromatic light. Broadband spectral illuminants determine the eye's sensitivity (Warrant and Nilsson 1998) and spatial resolution in real situations. The effective angular sensitivity then is calculated by integrating the absorbed light power together with the illumination spectrum as a function of incident angle, with subsequent normalization. This requires knowledge of the light spectrum as well as of the visual pigment's absorption spectrum. For most fly rhabdomere lengths this spectral averaging will reduce the deviations between the linear approximation and results of the full formalism.

Spectral sensitivity

The integral effective power for a given F-number is invariant for the facet lens diameter and only slightly dependent on wavelength; the spectral variation in the amplitude of the integral effective power is for each rhabdomere type only about 25% over a threefold F-number range (Fig. 9b). Minor troughs in the spectra occur at the wavelengths where modes are no longer bound by the rhabdomere, i.e. at about 325 nm of the 1-μm-diameter rhabdomeres and at 305, 410 and 650 nm for the other type (Fig. 9b). In reality these troughs will be less prominent, because unbound light is not accounted for, whilst it will contribute to light sensitivity. Especially in the case of the third mode, which becomes leaky above the cut-off wavelength, added sensitivity due to unbound light may not be fully negligible. Even when the smoothing of the spectra by leaky or unbound modes is extremely minor, the spectra of the effective power are rather flat compared to the characteristic bands of the absorption spectra of visual pigments (e.g., Stavenga et al. 1993). This means that the common practice of attributing measured sensitivity spectra completely to the visual pigment is largely correct for photoreceptor stimulations with an extended light source. However, with point light sources appreciable spectral modulations by the optics could result, especially in the slender rhabdomere photoreceptor type (Fig. 8b).

Anatomy shows that the effective diameter of the six R1–6 rhabdomeres of a retinula can vary somewhat. As

a consequence, the mode cut-off wavelengths vary, and the troughs in the integral effective power occur at different wavelengths. Because the signals of six different photoreceptors are summed by neurons in the lamina, the spectral sensitivity of these neurons will be strongly smoothed, resulting in a virtually flat spectrum.

Absolute light sensitivity

The rather limited dependence of the integral effective power on the F-number (Fig. 9a) has important consequences for the interpretation of the photoreceptors' absolute light sensitivity. An expression for the latter quantity, initiated by Kirschfeld (1974) and further developed by Land (1981, 1989) is:

$$S = S_o\left(1 - e^{-\kappa L}\right) \tag{5a}$$

where

$$S_o = \left(\frac{\pi}{4}\frac{D_l D_r}{f}\right)^2 = \left(\frac{\pi}{4}\frac{D_r}{F}\right)^2 = \left(\frac{\pi}{4} D_l \Delta\rho_r\right)^2 \tag{5b}$$

is a factor due to the optics; κ, the absorption coefficient of the visual pigment, is taken at the peak wavelength. Equation 5 has been used to compare the eyes of insects from different habitats in studies of insect eye design (Land 1981; Warrant and Nilsson 1998). Warrant and Nilsson (1998) have pointed out that it is more adequate to consider natural illuminants, and therefore they replaced the last factor in Eq. 5a, $[1-\exp(-\kappa L)]$, by a factor $\kappa L/(2.3+\kappa L)$, meaning a considerable linearization.

Although it is based on geometrical optics, Eq. 5 is quite similar to the expression for the light absorption derived from the wave optics model for the facet lens-rhabdomere system, Eq. A5 of Appendix 3. However, even within the geometrical optics realm, Eq. 5 cannot be applied to fly eyes without caution. The factor $D_l D_r/f$ in Eq. 5 assumes that all light projected by the facet lens within the cross-sectional area of the rhabdomere's tip is guided into the rhabdomere. Geometrical optics already tells us that this is only the case when $F \leq F_c$, the F-number value where rays through the lens are just totally reflected (Appendix 2 and Fig. 5), and the calculations based on wave optics corroborate this point (Fig. 8a, c). To investigate the validity of Eq. 5, the value of S_o (Eq. 5b) for the two rhabdomere types is presented in Fig. 11 by S_1 and S_2 (dotted curves), where again for D_r the value of the distal diameter of the rhabdomere is taken: $D_r = 1.0$ and 2.0 μm, respectively. It appears that Eq. 5 roughly predicts the absolute light sensitivity, but at low F-numbers large deviations of the data from the wave-optical model calculations occur (Fig. 11). Equation 5b can be partly rescued by accounting for the loss of the contribution of the marginal rays via:

$$S^* = \left(\frac{\pi}{4}\frac{D_r}{F^*}\right)^2 \tag{5c}$$

with $F^* = F_c$ when $F < F_c$ and $F^* = F$ when $F > F_c$, respectively; it is convenient to take $F_c = 2$, see

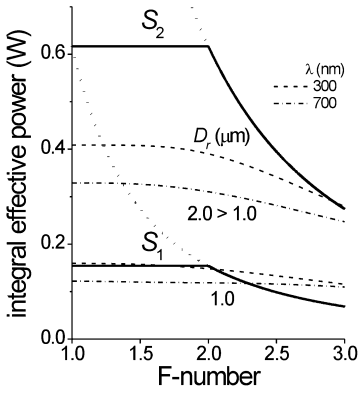

Fig. 11 Integral effective power for $\lambda = 300$ and 700 nm (see Fig. 9a) calculated with the wave optical model (Eq. A15) compared with related expressions for the light sensitivity based on geometrical optics (Eqs. 5b, 5c), for the two rhabdomere types, taking the distal rhabdomere diameters $D_r = 1.0$ and 2.0, respectively. The *dotted curves* S_1 and S_2 represent the uncorrected sensitivities (Eq. 5b), and the continuous curves include a correction for the leakiness of the rhabdomeres for low F-numbers, i.e., when $F < F_c = 2$ (Eq. 5c)

Appendix 2. This yields the horizontal lines for the sensitivities S_1 and S_2 (solid curves) in Fig. 11.

Land et al. (1999) calculated the sensitivity of the eyes of a number of mosquito species using Eqs. 5a, 5b. The optics and anatomy of the flies are different, but the sensitivities of lower and higher Diptera can be compared with the geometrical optics formalism of Eq. 5. However, because the mosquitoes have F-numbers much lower than 2, going even down to 0.78 (Land et al. 1999), the derived sensitivities need to be corrected for light leakage from the rhabdomeres.

The eye of *Drosophila*

Figures 7 and 8 show that the axial and integral light sensitivity change in opposite directions when the F-number increases, with a much greater loss of the sensitivity for an axial point source than the gain for an extended source. The remaining question then still is, why has *Drosophila* selected facet lenses with an F-number as small as $F = 1.25$. The sensitivity to point sources is strongly suppressed by both a small facet lens size and a low F-number (Fig. 8a, c), and the sensitivity to extended sources is about a meager 10–20% higher with $F = 1.25$ than with $F \approx 2.0$, preferred by the blowflies (Stavenga et al. 1990). The choice of a certain lens will depend on what has to be optimized: the absolute sensitivity for a point source or that for an extended source; of course, the sensitivity of a photoreceptor always will increase with the size of its rhabdomere.

For a given F-number, a crucial factor for the sensitivity to a point source is the facet lens area, but the sensitivity for an extended source does not change with facet lens size. Detection of a point source is best

achieved with an eye having high acuity and narrow angular sensitivities. Males of the larger flies realize that with expanded dorsal eye areas (for discussion, see van Hateren et al. 1989). Probably this is not a realistic option for *Drosophila* with its small head space. Compared to the bigger flies, the eyes of *Drosophila* occupy a large fraction of the head. The length of the truncated-cone shaped ommatidia is about 110 μm, which is a most considerable fraction of the eye's radius, $R = 180$ μm. Roughly, these figures are for the blowfly 300 μm and 1000 μm, respectively.

Evidently, the limited head space puts severe constraints to the construction of the eyes and hence limitations to their performance. Firstly, the wave properties of light put limitations on the diameter of the photoreceptors' rhabdomeres. With the open rhabdom structure, required in the neural superposition eye, the rhabdomeres together take up a considerable part of the ommatidial cross-section (Fig. 1), especially halfway down the retina where the rhabdomeres have strongly diverged. At least some extra space is needed, as the rhabdomeres contain the phototransduction system, which requires a heavy-duty support machinery located in the cell soma and the pigment cells. In addition, the pigment cells require space for pigment granules to act as a photoprotecting screen. It seems therefore that the *Drosophila* ommatidium, tapering from a diameter of 16 μm at the eye surface to 10 μm at the basement membrane, is very close to or at the limit necessary for a working neural superposition eye. Consequently, the interommatidial angle of $\Delta\phi = D_l/R$ cannot be made much smaller than 5.1°.

When the facet lens diameter is fixed at $D_l = 16$ μm, the choice of the F-number determines the image focal length, $f' = n'FD_l$. For $F = 2.0$ $f' = 42.9$ μm and for F $= 1.25$ $f' = 26.8$ μm, meaning a shortening of the focal length of 16.1 μm. Considering the total length of the retina, $L = 80$ μm, it may be wise to save such a distance from idle image space, i.e. to choose a small F-number. In addition to the argument of spatial economy, the consequences of a small F-number for the angular sensitivity may be even more important. Figure 10a, d shows that for a facet lens diameter of $D_l = 25$ μm at $F = 2.0$ $\Delta\rho \approx 1.5°$ for the slender rhabdomere type (D_r $= 1.0$ μm) and $\Delta\rho \approx 2.0°$ for the fatter type ($D_r = 2.0 >$ 1.0 μm). For $D_l = 16$ μm these values have to multiplied by 25/16, yielding 2.3° and 3.1° for the two rhabdomere types, respectively. These values are much smaller than the interommatidial angle $\Delta\phi = 5.1°$, leading to oversampling. For $F = 1.25$, Figure 10 gives scattered $\Delta\rho$-values around 1.8° and 2.7°, respectively, which for *Drosophila* mean 2.8° and 4.2°. Direct physiological measurements of the angular sensitivity of the photoreceptors to determine the validity of the present computational results are lacking. From optomotor responses, which presumably are driven by the peripheral photoreceptors, Götz (1964) derived $\Delta\rho = 3.5°$. Comparing this with the calculated 4.2° indicates that the diameter value used in the computations for the R1–6 rhabdomeres is slightly too large for *Drosophila*; indeed, 10–20% smaller rhabdomere values are found anatomically (Hardie 1985). It has to be mentioned in addition, that another cause of a smaller $\Delta\rho$ might have been the pupil mechanism. This system uses pigment granules in the photoreceptor soma which control the light flux in the rhabdomere (Franceschini 1975; Stavenga 1975). Stimulation of the photoreceptor with bright light causes narrowing of the angular sensitivity due to selective mode absorption by the closing pupil (Smakman et al. 1984).

In summary, the small F-number of *Drosophila* facet lenses is a good solution to the limits imposed by the head size on the facet diameter as well as on the length of the ommatidia. A small F-number is not bad either for the absolute light sensitivity. The facet lenses of the much larger houseflies and blowflies are often only slightly larger than those of *Drosophila*. The much larger radius of eye curvature allows small interommatidial angles, or high spatial resolution, necessitating narrow angular sensitivity curves, or small $\Delta\rho$-values, and thus a larger F-number than that of *Drosophila*.

Appendix 1

The thick fly facet lens

The power of a thick lens is given by (Jenkins and White 1976):

$$P_l = P_1 + P_2 + P_3 \tag{A1}$$

with

$$P_1 = \frac{n_l - n}{r_1}\ ,\ P_2 = \frac{n' - n_l}{r_2}\ ,\ \text{and}\ P_3 = -\frac{t}{n_l}P_1P_2 \tag{A2}$$

P_1 and P_2 are the powers of the front and back surface of the lens, respectively; r_1 and r_2 are the radii of curvature of front and back surface; t is the lens thickness; n, n_l and n' are the refractive indices of object space, lens, and image space, respectively (Fig. 2).

The primary or object focal length and the secondary or image focal length is given by, respectively:

$$f = \frac{n}{P_l}\ \text{and}\ f' = \frac{n'}{P_l} \tag{A3}$$

For a facet lens of *Drosophila* with $r_1 = 11$ μm, $r_2 =$ -11 μm, $t = 8$ μm, $n = 1.0$, $n_l = 1.45$, and $n' = 1.34$ follows $P_1 = 0.041$ μm^{-1}, $P_2 = 0.010$ μm^{-1}, $P_3 =$ -0.002 μm^{-1}, and $P_l = 0.049$ μm^{-1}, or, the lens power is mainly determined by the lens front surface. The object and image focal length then is $f = 20.6$ μm and $f' =$ 27.5 μm, respectively.

The geometrical optics of an imaging system is fully determined by its 6 cardinal points, i.e., the focal points F and F', the principal points H and H', and the nodal points N and N' (Fig. 3). The corresponding 6 cardinal planes are the planes through the cardinal points per-

pendicular to the optical axis. Points in one principal plane are imaged in the other principal plane with unit magnification. Rays in object space through the primary focal point F proceed in image space from the primary principal plane parallel to the optical axis, and rays in object space parallel to the optical axis proceed in image space from the secondary principal plane through the secondary focal point F'. Rays in object space through the primary nodal point N proceed in image space through the secondary nodal point N' in the same direction, i.e., the angle with the optical axis, θ, is identical for both rays. The distances of H and H' to the front surface are ntP_2/n_lP = 1.1 μm and $t(1-n'P_1/n_lP)$ = 1.8 μm, respectively, and the distances of N and N' to the back surface are $f'-t-n(1-tP_2/n_l)/P$ = 0.1 μm and $n'(1-tP_1/n_l)-f$ = 0.8 μm, respectively. The principal points (planes) as well as the nodal points (planes) virtually coincide: their identical distance is 0.7 μm (Figs. 2, 12; for the related case of the blowfly facet lens, see Stavenga 1975; Stavenga et al. 1990).

Figure 12 is added to emphasize how the geometrical optics of the fly facet lens determines two crucial aspects of the photoreceptor spatial sensitivity (see Land 1981). Firstly, the channeling of light into the rhabdomere depends on the size of the lens' exit pupil. Its size can be taken to be identical to that of the actual facet lens and its location to be that of the secondary principal plane. The angular aperture on the image side of the cone of light projecting at the rhabdomere thus is given by $2\theta_a = 2\ \mathrm{tg}^{-1}(D_l/2f')$; for a given D_l, the secondary or image focal length, f', is then the essential parameter (see Fig. 12a). Secondly, if the distal entrance of the rhabdomere coincides with the secondary focal plane, the visual axis and the photoreceptor's spatial field are determined by the position of the secondary nodal point. Here the primary or object focal length, f, is the essential parameter (Fig. 12b).

Fig. 12 Diagrams for illustrating the different functions of the principal planes, i.e., the planes through the principal points, H and H', and the nodal points, N and N'. F and F' are the focal points. For light focusing, the image focal length, f', is the essential parameter, and for the estimation of the visual axis and visual field, the object focal length, f, must be used

Appendix 2

Reflectance of the rhabdomere boundary

The reflectance of a boundary between two media with refractive indices n_1 and n_2 is given by Fresnel's reflection equations. For polarized light perpendicular and parallel to the plane of incidence the reflectances are given by, respectively:

$$R_s = \frac{\sin^2(\varphi_1 - \varphi_2)}{\sin^2(\varphi_1 + \varphi_2)} \text{ and } R_p = \frac{\mathrm{tg}^2(\varphi_1 - \varphi_2)}{\mathrm{tg}^2(\varphi_1 + \varphi_2)} \qquad \text{(A4)}$$

where the angles of incidence and refraction, ϕ_1 and ϕ_2, are related by Snell's law: $n_1\sin\phi_1 = n_2\sin\phi_2$. The values of R_s and R_p are virtually identical in the relevant range of small angles. Figure 5a gives the average reflectance, $R_r = (R_s + R_p)/2$, as a function of the rhabdomere refraction angle, θ_r. The critical angle for light reflection on the boundary of a fly rhabdomere is $\phi_c = \sin^{-1}(n_2/n_1) = 79.5°$, or, its complement $\theta_c = 10.5°$ (see Fig. 4a). $R_r = 1$ when $\theta_r < \theta_c$, but R_r rapidly becomes very minor when θ_r exceeds θ_c by more than a few degrees (Fig. 5a).

Figure 5b presents the relation between the facet lens F-number and the rhabdomere refraction angle, using $F = 1/(2n'\mathrm{tg}\theta_a)$ (see Eq. 1) and $\theta_a = \sin^{-1}[(n_1/n_2)\sin\theta_r]$. Let F_c be the critical value where $\theta_r = \theta_c$, then for $F \geq F_c$ all light rays focused by the facet lens into the rhabdomere will be reflected, but for $F < F_c$, rays from the lens periphery will leak out of the rhabdomere. The critical F-number, F_c, is used to rescue Land's (1981) expression for an eye's light sensitivity (Eq. 5). The chosen refractive index values yield $F_c = 1.98$. It could be argued that instead of taking the F-number corresponding to $\theta_c = 10.5°$, where the reflectance $R_r = 1$, it is better to take as the limiting F-number the value corresponding to the angle where $R_r = 0.5$: $\theta_r = 10.7°$. Then F_c would be $F_c = 1.94$ (Fig. 5). For convenience's sake the critical F-number here is approximated to $F_c = 2$.

Warrant and McIntyre (1993) state that the F-number where all light rays are just captured is about $F = 2.8$, but this number is estimated too large by a factor n', as the focal distances f and f' have been

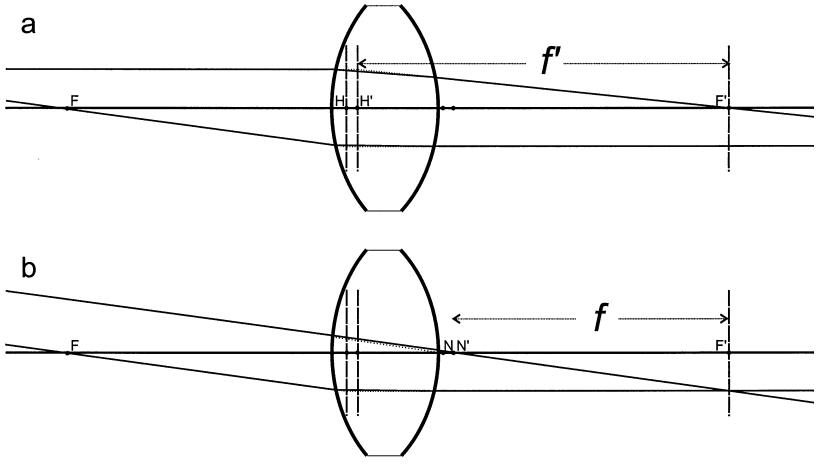

confused: for focusing light into the rhabdomere, *f'* and not *f* is the essential parameter; see Appendix 1.

When a parallel beam from a distant point source enters a *Drosophila* facet lens with $F = 1.25$, a marginal ray is given by $\theta_a = 16.6°$. The ray entering a rhabdomere with an angle $\theta_c = 10.5°$ makes an angle 10.7° with the visual axis. The ratio between the light power entering from the full angular aperture of the lens and that from a cone where all light rays are totally reflected is $(16.6/10.5)^2 = 2.4$. This means that well over half of the light rays are not captured by the rhabdomere. This largely explains the deviation of the sensitivities S_1 and S_2 (solid curves) in Fig. 11 from the integral effective power.

Appendix 3

Excitation of waveguide modes in a fly rhabdomere

Consider a facet lens-rhabdomere system illuminated by a distant point source from a directional angle θ (Fig. 3a). A total of 1 W of monochromatic light, wavelength λ, enters the facet lens, and is focused into the rhabdomere. The light power absorbed by the visual pigment then is (Stavenga 2003):

$$P_{abs}(\lambda) = \sum_p P_{p,exc}(\lambda)\left\{1 - e^{-\bar{\eta}_p(\lambda)\kappa(\lambda)L}\right\} \tag{A5}$$

where the sum is over the different modes; $P_{p,exc}$ is the power excited into mode p; $\bar{\eta}_p$ is the effective light fraction of mode p propagating inside the rhabdomere, from which the visual pigment molecules can absorb; $\kappa(\lambda)$ is the absorption coefficient of the rhabdomere medium due to the visual pigment; L is the length of the rhabdomere.

Equation A5 is considerably simplified when self-absorption by the visual pigment is minor. Then (Stavenga 2003, Eq. 44):

$$P_{abs}(\lambda) = \kappa(\lambda)\, L\, P_{eff}(\lambda) \tag{A6}$$

where P_{eff} is the effective light power from which light can be absorbed (Stavenga 2003, Eq. 45):

$$P_{eff}(\lambda) = \sum_p P_{p,exc}(\lambda)\bar{\eta}_p(\lambda) \tag{A7}$$

When the rhabdomere entrance coincides with the image focal plane of the facet lens, $P_{p,exc}$ is found from:

$$P_{p,exc} = \frac{2n_e}{c_p n' J_{l-1}(U) J_{l+1}(U)}\left[\frac{2}{C}\frac{W}{V}\int_0^C J_l(D\Omega)G(\Omega)\Omega d\Omega\right]^2 \tag{A8}$$

The five linearly polarized modes ($p = 1$–5) that are bound at wavelength 300 nm by a rhabdomere with diameter 2.0 μm are called LP01, LP11, LP21, LP02 and LP31 (see Table 2 of Stavenga 2003). For each mode, the value of l is the first of the number pair. When $l = 0$, $c_p = 1$, otherwise $c_p = 2$. U and W are roots of the waveguide characteristic equation:

$$U\frac{J_{l+1}(U)}{J_l(U)} = W\frac{K_{l+1}(W)}{K_l(W)} \tag{A9}$$

J_l and K_l are (modified) Bessel functions; n' is the refractive index of the facet lens image space (Fig. 2), and n_e is the effective refractive index of the rhabdomere. n_e and n' have very approximately the same value, or $n_e/n' = 1$. Furthermore, $D = (2FD_l/D_r)\mathrm{tg}\theta$; and C is an integration constant:

$$C = \frac{\pi D_r}{2\lambda F} \tag{A10}$$

$$G(\Omega) = \frac{V^2}{(\Omega^2 - U^2)(\Omega^2 + W^2)}[\Omega J_l(U)J_{l+1}(\Omega) - UJ_l(\Omega)J_{l+1}(U)]\ (\Omega = \mathrm{U}) \tag{A11a}$$

or

$$G(\Omega) = \frac{1}{2}\left[J_l^2(U) - J_{l-1}(U)J_{l+1}(U)\right]\ (\Omega = \mathrm{U}) \tag{A11b}$$

Finally, $\bar{\eta}_p$, the effective light fraction of mode p propagating inside the rhabdomere from which the visual pigment molecules can absorb is given by:

$$\bar{\eta}_p = \frac{1}{L}\int_0^L \eta_p(\lambda, z)dz \tag{A12}$$

where z is the longitudinal coordinate of the waveguide; η_p, the local light fraction inside the waveguide, is related to the waveguide number V and the corresponding U and W for mode p by:

$$\eta_p = \frac{W^2}{V^2}\left(1 - \frac{J_l^2(U)}{J_{l-1}(U)J_{l+1}(U)}\right) \tag{A13}$$

When the rhabdomere has a constant diameter, which is the case for the rhabdomeres of the central photoreceptors R7 and R8, $\bar{\eta}_p = \eta_p$. The rhabdomeres of the peripheral photoreceptors, R1–6, taper. The tapering is approximately parabolic in the housefly *Musca* (Boschek 1971): $D_r = D_r(0)[1\text{-}(z/L)^2/2]$, i.e., with a distal diameter $D_r(0) = 2.0$ μm, the proximal diameter, for $z = L$, is 1.0 μm. This parabolic tapering is assumed in Fig. 6b.

Appendix 4

Integral effective power due to an extended light source

When the facet lens-rhabdomere system is illuminated by a uniform light source with irradiance $Q(\lambda)$, the total light power excited in mode p is (e.g., Snyder 1979):

$$P_{p,\mathrm{int}}(\lambda) = 2\pi A_l Q(\lambda) \int_0^{\frac{\pi}{2}} \theta E_{p,exc}(\theta,\lambda)\mathrm{d}\theta \qquad \text{(A14)}$$

where $A_l = \pi D_l^2/4$ is the facet lens area, and $E_{p,exc}(\theta,\lambda)$ is the fraction of the light incident at the facet lens surface which is excited into mode p by light coming from an angle θ. $E_{p,exc}(\theta,\lambda)$ equals the dimensionless $P_{p,exc}(\theta,\lambda)$, as the latter is the excited light power when 1 W of monochromatic light enters the facet lens (see Appendix 3).

The integral effective light power then is, assuming negligible self-absorption (see Eq. A6 of Appendix 3):

$$P_{\mathrm{int}}(\lambda) = \sum_p P_{p,\mathrm{int}}(\lambda)\bar{\eta}_p(\lambda) \qquad \text{(A15)}$$

This quantity is independent of the facet lens diameter for a given F-number, because an increase in the facet lens diameter is fully compensated by the concomitant narrowing of the angular sensitivity function. In the calculations of the integral effective light power of Fig. 9, Q is taken as $Q = 1\ \mathrm{W\ sr^{-1}\ \mu m^{-2}}$ (μm because the dimension of the facet lens is μm).

The spectral sensitivity of a photoreceptor for an extended light source is calculated by normalization of the total light absorption by the visual pigment, which is obtained by multiplying P_{int} with the absorption coefficient $\kappa(\lambda)$ and length L (see Eq. A5 of Appendix 3).

References

Barrell KF, Pask C (1979) Optical fibre excitation by lenses. Optica Acta 26:91–108

Beersma DGM, Hoenders BJ, Huiser AMJ, Toorn P van (1982) Refractive index of the fly rhabdomere. J Opt Soc Am 72:583–588

Boschek B (1971) On the fine structure of the peripheral retina and lamina ganglionaris of the fly, *Musca domestica*. Z Zellforsch 118:369–409

Franceschini N (1975) Sampling of the visual environment by the compound eye of the fly: fundamentals and applications. In: Snyder AW, Menzel R (eds) Photoreceptor optics. Springer, Berlin Heidelberg New York, pp 98–125

Franceschini N, Kirschfeld K (1971a) Étude optique in vivo des éléments photorécepteurs dans l'oeil composé de *Drosophila*. Kybernetik 8:1–13

Franceschini N, Kirschfeld K (1971b) Les phénomènes de pseudopupille dans l'oeil composé de *Drosophila*. Kybernetik 9:159–182

Götz KG (1964) Optomotorische Untersuchung des visuellen Systems einiger Augenmutanten der Fruchtfliege *Drosophila*. Kybernetik 2:77–92

Hardie RC (1985) Functional organization of the fly retina. In: Ottoson D (ed) Progress in sensory physiology, vol 5. Springer, Berlin Heidelberg New York, pp 1–79

Hardie RC, Raghu P (2001) Visual transduction in *Drosophila*. Nature 413:186–193

Hateren JH van (1984) Waveguide theory applied to optically measured angular sensitivities of fly photoreceptors. J Comp Physiol A 154:761–771

Hateren JH van (1985) The Stiles-Crawford effect in the eye of the blowfly, *Calliphora erythrocephala*. Vision Res 25:1305–1315

Hateren JH van (1989) Photoreceptor optics, theory and practice. In: Stavenga DG, Hardie RC (eds) Facets of vision. Springer, Berlin Heidelberg New York, pp 74–89

Hateren JH van, Hardie RC, Laughlin SB, Stavenga DG (1989) The bright zone, a specialized dorsal eye region in the male blowfly *Chrysomia megacephala*. J Comp Physiol A 164:297–308

Jenkins FA, White HE (1976) Fundamentals of optics, 4th edn. McGraw-Hill, Auckland

Kirschfeld K (1967) Die Projektion der optischen Umwelt auf das Raster der Rhabdomere im Komplexauge von *Musca*. Exp Brain Res 3:248–270

Kirschfeld K (1974) The absolute sensitivity of lens and compound eyes. Z Naturforsch C 29:592–596

Kuiper JW (1965) On the image formation in a single ommatidium of the compound eye of Diptera. In: Bernhard CG (ed) The functional organization of the compound eye. Pergamon Press, Oxford, pp 35–50

Land MF (1981) Optics and vision in invertebrates. In: Autrum H (ed) Handbook of sensory physiology, vol VII/6B. Springer, Berlin Heidelberg New York, pp 472–592

Land MF (1989) Variations in the structure and design of compound eyes. In: Stavenga DG, Hardie RC (eds) Facets of vision. Springer, Berlin Heidelberg New York, pp 90–111

Land MF, Nilsson D-E (2002) Animal eyes. Oxford University Press, Oxford

Land MF, Gibson G, Horwood J, Zeil J (1999) Fundamental differences in the optical structure of the eyes of nocturnal and diurnal mosquitoes. J Comp Physiol A 185:91–103

McIntyre PD, Kirschfeld K (1982) Chromatic aberration of a dipteran corneal lens. J Comp Physiol A 146:493–500

Pask C, Barrell KF (1980a) Photoreceptor optics I: introduction to formalism and excitation in a lens-photoreceptor system. Biol Cybern 36:1–8

Pask C, Barrell KF (1980b) Photoreceptor optics. II. Application to angular sensitivity and other properties of a lens-photoreceptor system. Biol Cybern 36:9–18

Seitz G (1968) Der Strahlengang im Appositionsauge von *Calliphora erythrocephala* (Meig.). Z Vergl Physiol 59:205–231

Smakman JG, Hateren JH van, Stavenga DG (1984) Angular sensitivity of blowfly photoreceptors: intracellular measurements and wave-optical predictions. J Comp Physiol A 155:239–247

Snyder AW (1979) Physics of vision in compound eyes. In: Autrum H (ed) Handbook of sensory physiology, vol VII/6A. Springer, Berlin Heidelberg New York, pp 225–313

Stavenga DG (1975) Optical qualities of the fly eye—an approach from the side of geometrical, physical and waveguide optics. In: Snyder AW, Menzel R (eds) Photoreceptor optics. Springer, Berlin Heidelberg New York, pp 126–144

Stavenga DG (2003) Angular and spectral sensitivity of fly photoreceptors. I. Integrated facet lens and rhabdomere optics. J Comp Physiol A 189:1–17

Stavenga DG, Hateren JH van (1991) Focusing by a high power, low Fresnel number lens: the fly facet lens. J Opt Soc Am A 8:14–19

Stavenga DG, Kruizinga R, Leertouwer HL (1990) Dioptrics of the facet lenses of male blowflies *Calliphora* and *Chrysomia*. J Comp Physiol A 166:365–371

Stavenga DG, Smits RP, Hoenders BJ (1993) Simple exponential functions describing the absorbance bands of visual pigment spectra. Vision Res 33:1011–1017

Warrant EJ, McIntyre PD (1993) Arthropod eye design and the physical limits to spatial resolving power. Prog Neurobiol 40:413–461

Warrant EJ, Nilsson DE (1998) Absorption of white light in photoreceptors. Vision Res 38:195–207

Wijngaard W, Stavenga DG (1975) On optical crosstalk between fly rhabdomeres. Biol Cybern 18:61–67